

RESEARCH

Open Access



Development of nanospray loaded with ciclopirox for dermal fungus treatment: determination of pro-inflammatory interleukin IL-2 mRNA expression

Yasir Mehmood¹, Hira Shahid², Rabbia Nazir³, Mohammad N. Uddin⁴, Mohammad Nur-e-Alam^{5*}, Mohammed Bourhia^{6*}, Khalid S. Almaary⁷, Mohsin Kazi⁸ and Ousman B. Mahamat^{9,10}

Abstract

The aim of this study was to develop a ciclopirox (CXP) topical nano spray using nanotechnology to enhance drug bioavailability and skin absorption. A precipitation method was employed to incorporate CXP in its nano particulate form, using chitosan as the polymer. Chitosan nanoparticles (CT NPs) possess unique properties that make them highly suitable for biological applications. The study focused on investigating the penetration behavior of chitosan nanoparticles (nano spray) through artificial skin, with the goal of developing them as effective skin delivery systems for medications. The nanoparticles had an average size of 640 nm, with a positive or negative surface potential and a polydispersity index (PDI) of 0.298. A thorough analysis of the nano spray was conducted using several scientific techniques, including X-ray diffractometry, scanning electron microscopy, Fourier transform infrared spectroscopy, differential scanning calorimetry (DSC), as well as in vitro release and diffusion studies. Additionally, cell viability was evaluated using the MTT assay, and blood compatibility was tested through a hemolysis test. The study also assessed the levels of the anti-inflammatory cytokine IL-2 in the lungs of mice using RNA extraction, reverse transcription, and polymerase chain reaction (RT-PCR). The drug dissolution and diffusion rates showed a significant improvement compared to the pure reference sample. Therefore, the CXP nano spray appears to be an efficient and practical method to enhance skin penetration, bioavailability, and permeability. Based on the results, the CXP nano spray holds potential as a promising treatment for fungal infections, particularly for skin diseases.

Keywords In vitro, Diffusion, Diameter, Cytokines, Diffusion, Skin penetration

*Correspondence:

Mohammad Nur-e-Alam
mohalam@ksu.edu.sa
Mohammed Bourhia
bourhia.mohamed@gmail.com

Full list of author information is available at the end of the article



© The Author(s) 2025. **Open Access** This article is licensed under a Creative Commons Attribution-NonCommercial-NoDerivatives 4.0 International License, which permits any non-commercial use, sharing, distribution and reproduction in any medium or format, as long as you give appropriate credit to the original author(s) and the source, provide a link to the Creative Commons licence, and indicate if you modified the licensed material. You do not have permission under this licence to share adapted material derived from this article or parts of it. The images or other third party material in this article are included in the article's Creative Commons licence, unless indicated otherwise in a credit line to the material. If material is not included in the article's Creative Commons licence and your intended use is not permitted by statutory regulation or exceeds the permitted use, you will need to obtain permission directly from the copyright holder. To view a copy of this licence, visit <http://creativecommons.org/licenses/by-nc-nd/4.0/>.

Introduction

The skin, our body's largest organ, serves a multitude of functions. Every year, a significant amount of resources are dedicated to addressing skin injuries, including pressure sores, ulcers, burns, and various types of wounds caused by abrasion or trauma [1]. As a result, a significant amount of research is being conducted on wound dressings to develop an effective strategy for enhancing wound healing [2]. An important obstacle to the healing of wounds is infections caused by bacteria, fungi, and other microorganisms found in the affected area of the skin [3]. Complications can occur due to this microbial infection, leading to prolonged healing of the skin. This highly contagious condition may result in delays in skin healing [2].

In Asian and African nations, approximately 15% of the population has common fungal infections, including dermatophytes and candidiasis. This highlights the significant occurrence of such conditions in these regions [4]. With limited effectiveness, lower than ideal minimum inhibitory concentration (MIC) values, increased side effects, and increased drug resistance associated with some current antifungal drugs, there is a growing search for innovative antifungal treatments [5]. Efforts have been redirected toward the development of transdermal antifungal treatments to combat fungal pathogens, which is quite remarkable. Using the skin as a pathway for drug administration offers numerous benefits, such as minimizing side effects, maintaining consistent drug delivery, providing a noninvasive method of application, being user friendly, and allowing for easy discontinuation of medication. However, the issue remains in topical drug delivery, as the skin acts as a natural barrier to drug transport, and the process of drug movement through the skin is complex [6].

Ciclopirox (CXP) is an FDA-approved drug that has proven to be effective against fungi. It works by utilizing its metal chelation properties and engaging various molecular mechanisms [7]. Ciclopirox (CXP) is a highly effective antimycotic agent known for its ability to inhibit metal-dependent enzymes involved in the breakdown of harmful peroxides [8]. Ciclopirox, an antifungal agent from the hydroxypyridone class, has a unique structure that separates it from common imidazole derivatives and other antifungal compounds. Ciclopirox, an antifungal agent of the hydroxypyridone class, has a unique structure that separates it from common imidazole derivatives and other antifungal compounds [9].

The effectiveness of a drug in a clinical setting depends on its ability to penetrate the stratum corneum (SC) [10]. The stratum corneum (SC) offers a range of accessible and advantageous features, making it a promising avenue for delivering therapeutic agents and addressing both local and systemic effects. The human skin is a

remarkable and efficient barrier that is designed to protect and repair itself, ensuring internal well-being and resilience against external factors [11].

The use of cutting-edge technology to deliver specific therapeutic agents has prompted researchers to develop a number of novel drug delivery methods for topical use. Ensuring the accurate delivery of active agents at defined rates and targeting particular areas in line with physiological needs has contributed significantly to keeping the active ingredient ratio within the therapeutic range [12]. A variety of potential drug delivery systems exist, including liposomes, nanoparticles, dendrimers, niosomes, microspheres, microneedles, and micelles. These different techniques have the potential to advance and refine medication delivery strategies [13]. The market offers a wide range of alternatives for treating fungal infections in various dose forms. Creams remain the principal form, with ciclopirox available in a variety of concentrations. A growing star in this field is the topical spray, which provides a simple method of administration to afflicted regions. This spray provides a simple yet efficient technique for controlling cutaneous fungal infections, especially those affecting the scalp and nails [14].

Chitosan (CS), a carbohydrate polymer, has received significant interest in a variety of industries because of its unique properties, such as biodegradability, biocompatibility, and ease of availability. Its distinguishing characteristics make it a focus point for substantial investigation across several fields [15, 16]. Chitosan is mainly sourced from the abundantly occurring natural polymer, chitin, through the process of deacetylation. Studies evaluating the therapeutic use of chitosan have consistently reported satisfying levels of safety and biocompatibility, including in the human skin cells [17]. Furthermore, the innate ability of chitosan to disintegrate spontaneously; its compatibility with living tissues; and its anti-infective, antibacterial, and hemostatic properties contribute to its versatility in a wide range of biobased and biomedical applications [18]. In this research we have prepared nano spray contain CXP for fungus treatment. We have chitosan polymer which was used in several skin delivery systems to enhance the drug penetrations into skin [17]. Physicochemical properties of the developed nanoparticles (nano spray) including particle size, charges, PDI, surface morphology, cytotoxicity were evaluated. We also evaluated the permeation properties of the chitosan nanoparticles using artificial skin to track the permeation pathways of the nanoparticles through the skin.

Materials and methods

Chemicals

Saffron Pharmaceuticals, a trustworthy provider based in Faisalabad, Pakistan, generously supplied ciclopirox (CXP). The Houston, Texas, USA-based Spectrum

Medical Industries supplied the dialysis membranes with an 8000 Da molecular weight cutoff (MWCO). An established Korean supplier, Dae-Jung Chemicals, was contacted to acquire 95% ethanol and 80% polylobate. The chitosan (CS) was sourced from the prestigious pharmaceutical company Merck and has a CAS number of 9012–76–4. Water that was double distilled on site was used throughout the whole course of the experiments. Acetonitrile, glacial acetic acid, and acetylacetone were among the additional solvents and reagents that were acquired from Dae-Jung Chemicals in Korea. They were of analytical-grade purity. The testing techniques were guaranteed to be reliable and precise owing to this extensive assortment of high-quality chemicals and materials.

Nano spray preparation

A nano spray using chitosan was created by making slight adjustments to the well-known nanoprecipitation technique. In the initial step, a solution of chitosan (CS) was created by combining 500 mg of chitosan with 100 mL of aqueous acidic solution (pH < 6.5) at a temperature of 50 °C and stirring at 2000 RPM. After stirring for 15 min, a small amount of ethanol (10 mL) was slowly added to the chitosan solution. The pH was then adjusted to 5.5 by adding a NaOH solution while keeping the temperature at 50 °C and stirring at 2000 RPM. On the basis of the provided conditions, a solution was created by mixing CXP with ethanol and stirring vigorously [19, 20]. The CXP solution and polymer solution were injected into 20 mL of distilled water containing 0.5% w/v Tween 80 at a consistent rate (0.1 mL/min) via a 26-gauge syringe. The mixture was carefully blended for two hours at a consistent agitation speed of 2000 rpm via a magnetic stirrer. Later, the suspension underwent sonication with the help of an ultrasonic probe sonicator (ZHANYI Sonic, China). The solution was diluted with phosphate buffer (pH 5.5) and then transformed into a spray by pouring it into appropriate containers [21, 22]. We have prepared different formulations with changings in polymer concentration. We have used different concentrations of polymers and observe the drug loading and encapsulations and select the best formulation. The findings of the drug entrapment experiment are shown in Table 1. CXP-NS-3 formulation which contained 0.66% chitosan

showed the greatest drug entrapment and loading when the drug entrapment and loading was assessed. In this investigation, the selected formulation was further characterized. The HPLC technique was used to determine the amount of CXP that was trapped in the nano particles. The CXP nano spray was found to have a quantity of CXP that was similar to that of CXP-NS-3. When a low amount of chitosan is used in the formulation, the number of available sites for drug encapsulation may be insufficient. Chitosan, being a biopolymer with hydrophilic and charged functional groups, is responsible for forming the nanoparticle matrix that encapsulates the drug. At lower concentrations, the polymeric network may not be dense enough to hold a significant amount of drug within its structure, resulting in lower entrapment efficiency and drug loading. Additionally, the lower viscosity of the chitosan solution at reduced concentrations might lead to poorer formation of nanoparticles, affecting the ability to encapsulate the drug efficiently. On the other hand, when a high amount of chitosan is used, the particle size might increase due to the excess polymer forming larger aggregates. This can lead to poor drug distribution within the particles, causing some of the drug to remain unencapsulated or in excess in the external phase, rather than being entrapped inside the nanoparticle matrix. Additionally, at higher chitosan concentrations, the increased viscosity of the solution could hinder efficient drug diffusion into the nanoparticle network during formulation, resulting in lower drug entrapment.

Determination of drug entrapment efficiency and loading capacity

To facilitate the formation of nanoparticle precipitates, the ethanol-mixed nano spray was subjected to centrifugation at 2000 rpm for 30 min. After that, the mixture was collected again, mixed with ethanol, and vigorously shaken on a vortex for one minute. The solution was carefully filtered and then mixed with the mobile phase before being analyzed for CXP concentration via a reliable HPLC technique.

The HPLC system used was a Shimadzu LC 20AB equipped with a 1000 pump and UV-VIS detector from Japan. A column with dimensions of 250×4.6×5 mm was utilized as the stationary phase, while the mobile phase consisted of a blend of water, acetonitrile, glacial acetic acid, and acetyl acetone in specific proportions. The UV detector was configured to function at a wavelength of 298 nm, utilizing an injection volume of 20 µL and a mobile phase flow rate of 1.0 mL/min. An extensive analysis was performed by comparing the obtained chromatograms to those of the standard [23]. In addition, a thorough calculation of drug loading efficiency was conducted three times. In addition, the nano spray actuator stability and uniformity were evaluated via the same

Table 1 Drug entrapment efficiency and loading (all formulations)

Code	Drug Entrapment Efficiency CXP %	Drug loading Efficiency CXP %
CXP-NS -1	49.21 ± 3.7	24.11 ± 1.5
CXP-NS -2	52.82 ± 1.6	41.32 ± 2.4
CXP-NS -3	78% ± 5.2	53% ± 1.23
CXP-NS -4	61.36 ± 1.3	61.39 ± 4.5
CXP-NS -5	51.81 ± 2.9	53.82 ± 2.5

method. However, these measurements were not carried out in this particular project. The entrapment effectiveness and drug loading of the prepared particles for Roflumilast has been calculated using the following Eqs. (1 and 2).

$$\text{Entrapment efficiency \%} = \frac{\text{Weight of the drug in particles}}{\text{Weight of particles}} \times 100 \quad (1)$$

$$\text{Entrapment efficiency \%} = \frac{\text{Drug added} - \text{Free drug}}{\text{Drug added}} \times 100 \quad (2)$$

Particle size, polydispersity index (PDI) and zeta potential

The particle size, polydispersity index (PDI), and zeta potential were measured via a particle size analyzer and photon correlation spectroscopy (PCS) with a Zetasizer device made by Malvern Instruments, UK. The process involved preparing a CXP nano spray solution by diluting it in filtered water and then immediately using it to evaluate the polydispersity index (PDI) and particle diameter [24].

FTIR spectroscopy

The FTIR spectrometer utilized in this investigation was a Thermo Scientific Nicolet iN5 FTIR instrument manufactured in the United States and equipped with an attenuated total reflection crystal cell. A minute quantity of each sample was administered to the instrument via a spatula and subsequently compacted with force. Spectra in the 800–4000 cm^{-1} range were captured via this approach for CXP, CS, and CXP nano spray [25].

Thermal analysis DSC study

Scanning calorimetry was conducted on CXP, CS, and CXP nano spray via Diamond Series DSC equipment from Perkin Elmer, USA. The procedure involved placing the samples into standard empty aluminum pans and conducting temperature scans ranging from 25 to 300 °C. A control pan without any contents was subjected to the same heating procedure as a blank reference. A constant inert atmosphere was maintained, and nitrogen purging was applied at a flow rate of 20 mL/min [26].

XRPD analysis

The CXP, CS, and CXP nano sprays were analyzed via a DADVANCE X-ray powder diffraction analyzer, a German instrument made by Bruker. Using $\text{Cu K}\alpha$ radiation (1.542 Å) in the 5 to 50 2θ range, with increments of 0.02 and a scan step time of 2.00 s, the apparatus functioned at 30 kV and 15 mA. After this, the data that had been collected were analyzed and are presented as the peak height (intensity) relative to 2θ [27].

Morphology study (SEM)

A JEOL Ltd. scanning electron microscope, located in Tokyo, Japan, was used to conduct the morphological examination. Metal stubs covered with gold and double-sided sticky tape held both the crystal form of the CXP raw powder and the CXP nano spray, which were then examined [28].

In-vitro release study

Both the nano spray and CXP were subjected to in vitro testing via the dialysis membrane method. The medication was combined with 5 mL of distilled water and placed in a dialysis bag from Medicell International Ltd. The bag was securely sealed to contain 1 mg of a specialized spray. A phosphate buffer solution with pH values of 5.5 and 7.4 was added to 500 mL of medium, which was maintained at 37.0 °C and stirred constantly at 50 rpm. Every enclosed bag was subsequently suspended in this solution. These two pH values were chosen to mimic the drug release and diffusion process in a situation that resembles the pH of the skin (approximately 5–6) and a skin wound that is infected, potentially leading to an elevated pH (7–8) [29].

Under consistent conditions, a 2.0 mL sample was periodically extracted and substituted with a new 2.0 mL sample. The filtrate was collected with a 0.45 μm pore size and subsequently diluted in the mobile phase for HPLC analysis. During the technique validation trials, a calibration curve was successfully developed with a remarkable level of accuracy ($R^2 = 0.998$; Zhang et al., 2010). A curve was used to determine the drug concentration in the resulting sample. A calculation was employed to ascertain the percentage release (3) [30, 31].

$$\text{Drug release percentage} = \frac{\text{sample absorbance}}{\text{standard absorbance}} \times 100 \quad (3)$$

In-vitro diffusion studies

This study employed a silicon membrane to evaluate permeability in vitro via a Franz diffusion cell. This study aimed to assess the permeability of a CXP nano spray and a commercially available cream by using a silicon membrane. The vertical Franz diffusion cell used, produced by SES Analytical Systems, GmbH, Germany, had a receptor volume of 5.2 mL and a donor surface area of 1.2 cm^2 . The donor and receptor chambers of the Franz diffusion cell were separated by a semisynthetic silicon membrane. The membrane, manufactured by SAMCO in Nuneaton, UK, was positioned with its epidermal side facing upward. A sample of the nanos spray was introduced into the donor chamber, which was coated with paraffin. The pH of the receptor chamber in the circulating water system was only 5.5, and the temperature was 37 ± 0.5 °C. Prior to the experiment, the temperature was

carefully regulated at 37 ± 0.5 °C, and the membrane was delicately positioned in contact with the receptor phase. After a period of 120 min in the receptor phase, 0.5 mL samples were collected at regular intervals and analyzed at 298 nm via a UV spectrophotometer. Afterward, a buffer solution with an equivalent concentration was introduced into the cell [32, 33].

In vitro cell viability studies

When conducting in vitro research, it is crucial to assess cell viability or cytotoxicity, particularly when examining substances such as pesticides and pharmaceuticals. These substances play a role in causing cell death through various cytotoxic mechanisms. Various mechanisms include damage to cell membranes, interruption of protein synthesis, and the creation of permanent receptor connections. It is evident that cytotoxicity is a multifaceted concept in biological assessments, given the intricate interplay of numerous processes. We utilized this method during our investigation of the CXP nano spray. For culture, researchers have utilized the HepG2 cell line, which is derived from human liver cells. I acquired this line from the ATCC via the University of Lahore. We utilized the MTT test, a widely recognized method for evaluating cell viability and proliferation, which was introduced by Mosmann in 1983. Our aim was to investigate the mitochondrial activity of succinate dehydrogenase prior to the administration of the nano spray [34].

The cell medium was subjected to different concentrations of nano spray (50, 100, 150, and 200 µg/mL) for a period of 24 h. After the incubation period, a 15 µL solution of MTT (5 mg/ml) in PBS was added to each well and then incubated for an additional 4 h at 37 °C. Afterwards, we meticulously removed the media containing MTT by aspiration. Next, we used 100 µL of dimethyl sulfoxide (DMSO) to dissolve the formazan crystals that had formed in each well. Following the procedure described by Patel, Gheewala, Suthar, and Shah in 2009, a microplate reader was used to measure the absorbance of the dissolved formazan crystals at 570 nm. We employed a calculation method to determine the percentage of viable cells [27].

$$\% \text{ cell Viability} = \frac{\text{Abs of treated cell} - \text{Abs of blank}}{\text{Abs of Control} - \text{Abs of Blank}} \times 100 \quad (4)$$

Hemolytic investigations

To carry out the hemolytic analysis, human blood was placed in a tube and then subjected to centrifugation at 1500 rpm for 5 min using ethylene diamine tetraacetic acid (EDTA). Next, the liquid above was carefully poured out, and the solid below was rinsed three times with PBS. The mixture was vigorously mixed for a brief period following the addition of 3.8 mL of phosphate-buffered

saline to 200 µL of the washed blood sediment. Following the process of heating the samples to 37 °C for 2 h, they were then spun at 1600 rpm for 5 min in a centrifuge. We measured the absorbance of the supernatant at 541 nm. For this experiment, we selected phosphate-buffered saline as the negative control and filtered water as the positive control. We utilized Eq. (5) to calculate the extent of hemolysis. In 2018, Assadi and colleagues published a paper on the subject. The study received approval from the ethical commission (IRB NO: RLCP/197/2023).

$$\% \text{ Hemolysis} = \frac{\text{ABS sample} - \text{ABS blank}}{\text{ABS positive} - \text{ABS blank}} \times 100\% \quad (5)$$

Effects on the expression levels of proinflammatory cytokines

In this study, we focused on the role of interleukin-2 (IL-2), a proinflammatory cytokine mostly produced by lymphocytes, in the development of allergic asthma. We divided 30–50 g mice into four groups and used them to study this phenomenon. Our method involved the delivery of ovalbumin after intraperitoneal sensitization to induce cytokines. A total of 20 g of ovalbumin dissolved in an aluminum hydroxide solution was added to the peritoneum of each group on days 0 and 14, except for the control group, which received 2 mg of ovalbumin dissolved in 0.1 ml of phosphate-buffered saline. The RLCP Ethical Review Board approved all the experimental procedures, and the study adhered to the ethical principles outlined in the Declaration of Helsinki by the World Medical Association. As part of the study, the animals were only exposed to phosphate buffer solution challenges after being subjected to simulated sensitization; these animals served as a control group. After 14 days, the two groups of mice were administered varying doses of CXP Nano spray or a pure drug mixture. The dosages were determined on the basis of the human dose and adjusted for the weight of the animals [35].

As an additional component of their treatment, certain mice received ovalbumin on a daily basis. After the 28-day period, the groups were allowed to sleep, and the TRIzol technique was used to extract total RNA from the lung samples. On the basis of the methodology and reaction parameters described in our previous publications, we successfully determined the total RNA yield and purity [36]. Following synthesis, the cDNA was incubated at 42 °C for 60 min and subsequently stored at -20 °C. Using the cDNA as a template, we conducted polymerase chain reaction amplification with primers specific to the gene [37].

Antifungal study

The antifungal activity of the nano spray against *Aspergillus niger* was tested in vitro via the agar well diffusion

technique. A 100 mL flask of Sabouraud dextrose agar (SDA) was divided into twenty-millilitre (mL) portions and then evenly and smoothly distributed into sterile glass Petri plates. After the petri dishes had hardened, they were split into the middle and marked as either a sample or standard. The Petri dishes were then filled with 50 mL of medium that contained a suspension of *Aspergillus niger*. After being accurately measured, the samples were dissolved in sterile water and placed into the corresponding holes, which were used as reference standards and samples. Nano spray samples and the standard were added. After the holes were filled, the plates were placed in a cold incubator at $22\text{ }^{\circ}\text{C} \pm 2\text{ }^{\circ}\text{C}$ for at least 24 h with the lids on top [38].

Using a Vernier caliper, we measured the inhibition zone on the plates in millimeters after the incubation time ended. A predetermined algorithm was used to determine the outcomes (6).

$$\% \text{ age of AM} = \frac{A2 \times W1 \times P}{A1 \times W2} \quad (6)$$

A1 = Area of zone of inhibition (mm) for standard.

A2 = Area of zone of inhibition (mm) for sample.

W1 = Weight of working standard.

W2 = Weight of sample.

P = Potency of working standard in %.

Analytical statistics

GraphPad Prism v.5 was used for statistical analysis, which included one-way analysis of variance (ANOVA) and Tukey's test. The standard deviation (SD) and mean were used to depict the data. The threshold for statistical significance was set at a P value of 0.05.

Results

A broad array of particles with sizes typically ranging from 1 to 1000 nm make up what is known as nanoparticles (NPs). A variety of forms and architectures are possible for these particles, including cylindrical, spherical, tubular, conical, and spiral. Owing to their low toxicity, ability to cross several biological barriers, and ability to covalently conjugate with hydrophobic medicines, these materials are also promising therapeutic choices. A modified precipitation process was employed to make the CXP nano spray. For topical usage, scientists created CXP nano sprays to increase solubility and penetration. The percentages and mg concentrations of various components are displayed in Table 1. The study demonstrated that the nanoparticles loaded with CXP exhibited promising drug entrapment and loading efficiencies. The entrapment efficiency was found to be $78\% \pm 3.5$, indicating that a substantial proportion of the drug was successfully encapsulated within the nanoparticles. Additionally, the drug loading capacity was $53\% \pm 1.43$, reflecting a relatively high amount of CXP incorporated into the particles compared to the total weight. These results suggest that the prepared nanoparticles have significant potential for effective drug delivery, with good encapsulation and loading efficiency, making them suitable for further development in therapeutic applications.

Particle size, polydispersity index (PDI), and Zeta potential

The CXP nano spray charge, size distribution, and size were determined via DLS. Figure 1 shows a graphic showing the distribution of sizes for the CXP nano sprays generated in water. Nano spray measurements via DLS revealed a PDI of 0.298 and a hydrodynamic diameter of 640 nm. At a temperature of $25 \pm 0.5\text{ }^{\circ}\text{C}$, the zeta potential of the nanospray was measured via a Malvern Zetasizer ZS200. Every sample underwent a minimum of three measurements. Fully stabilizing the system was achieved,

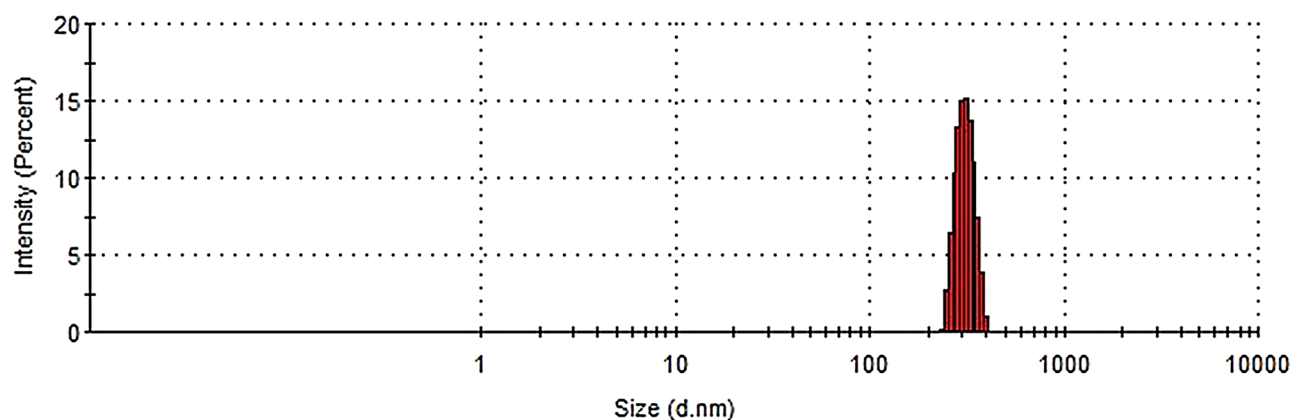


Fig. 1 Size distributions and charge of the CXP nano spray

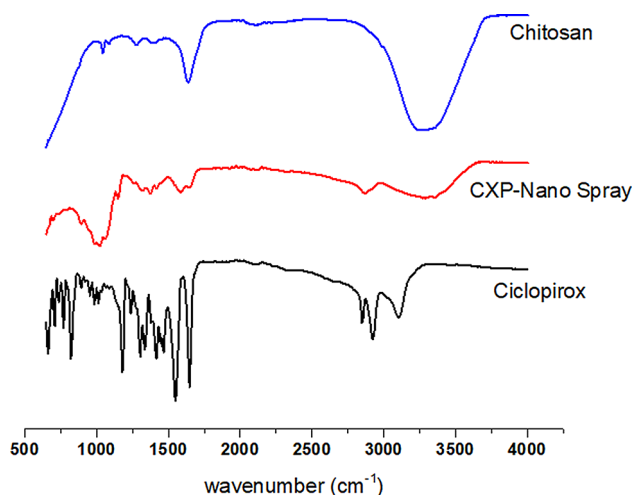


Fig. 2 FTIR analysis of the CXP, chitosan, and CXP nano spray

with an average value of -12 mV for the CXP nano spray zeta potential.

FT-IR analysis

Figure 2 shows the results of an investigation into the functional groups present in the synthesized CXP nano spray via Fourier transform infrared spectroscopy in the $800\text{--}4000\text{ cm}^{-1}$ range. A peak at 1631.17 cm^{-1} , which is indicative of the amide group of the drug, is observed in the spectrum of pure CXP. While peaks between 1000 and 1700 cm^{-1} are the most common, N=N stretching causes two more noticeable peaks at 1570 and 1690 cm^{-1} [39].

Upon examining the infrared spectra of natural chondroitin, we identified a number of distinct bands. There is a noticeable band at 3400 cm^{-1} , indicating the occurrence of O-H and N-H bond stretching vibrations. In this scenario, the stretching vibrations of the N-H bonds align with those of the O-H bonds. The peak at 2900 cm^{-1} is caused by the symmetrical and asymmetrical stretching vibrations of the C-H bonds in the -CH₂ and -CH₃ groups of the aliphatic chains. The peak at 1225 cm^{-1} is commonly observed in chondroitin sulfate and is attributed to the stretching vibrations of certain bonds. The spectra (Fig. 2) clearly demonstrate the effectiveness of the CXP nano spray in concealing the distinct peaks of CXP. Several peaks are observed in the spectrum, specifically at 1334 cm^{-1} , 1671 cm^{-1} , and 1599 cm^{-1} . These peaks correspond to different vibrational and stretching modes. There was a minor alteration in the peak intensities of C-H and O-H. The peak at 2900 cm^{-1} shifted to 3000 cm^{-1} , whereas the peak at 3490.99 cm^{-1} shifted. On the basis of the fluctuations in peak intensity observed during the formation process of the nano spray, it can be concluded that there was limited interaction between

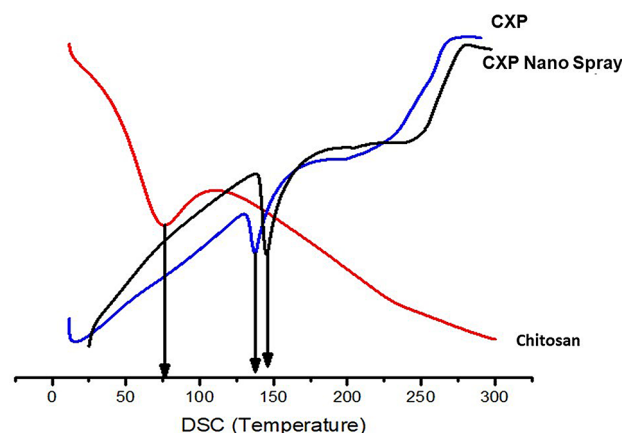


Fig. 3 Thermal analysis of the CXP, CS and CXP nano pray

CXP and the CS polymer. Through this interaction, the polymer efficiently captured CXP.

Thermal analysis

The CXP nano spray, together with the CS and CXP, were evaluated via the Q-2000 thermal analysis model developed by TA USA. The temperature may be adjusted from 0 to 300 degrees Celsius at a rate of 20 degrees Celsius each minute. The response of the CXP nano spray, SC, and CXP to heat flow is depicted in Fig. 3. This may determine the characteristics of the DSC. Figure 3 displays the results of the DSC examinations of the CXP, SC, and CXP nano sprays. As shown in Fig. 3, the DSC curve of CXP exhibited an exothermic peak at $60\text{ }^{\circ}\text{C}$ as a result of the partial loss of residual humidity. At approximately $240\text{ }^{\circ}\text{C}$, there is an exothermic peak caused by the glass transition temperature (T_g). The complex thermal reactions that take place at approximately $240\text{ }^{\circ}\text{C}$ make it quite evident that CXP melts significantly.

Morphology analysis (SEM)

The electron microscope's particle scanning capabilities verified that the CXP nano spray was indeed spherical. Figure 4 displays identical results for an improved nano spray formulation, as shown in Fig. 4, whereas Fig. 5 displays scanning electron microscopy (SEM) micrographs of pure CXP. The chaotic shape of the CXP nano spray might be explained by phase evaporation that occurs during particle hardening. The controlled release capabilities of the drug particles contained in this CXP nano spray make it a crucial aspect of the delivery system [9]. The particle distribution was shown to be uniform in the CXP nano spray via the scanning electron micrographs (SEMs) shown in Fig. 4B, and C. The findings revealed an efficient nano spray with API crystalline particles, which revealed a nonordered structure, as shown in Fig. 4A, featuring large crystal particles.

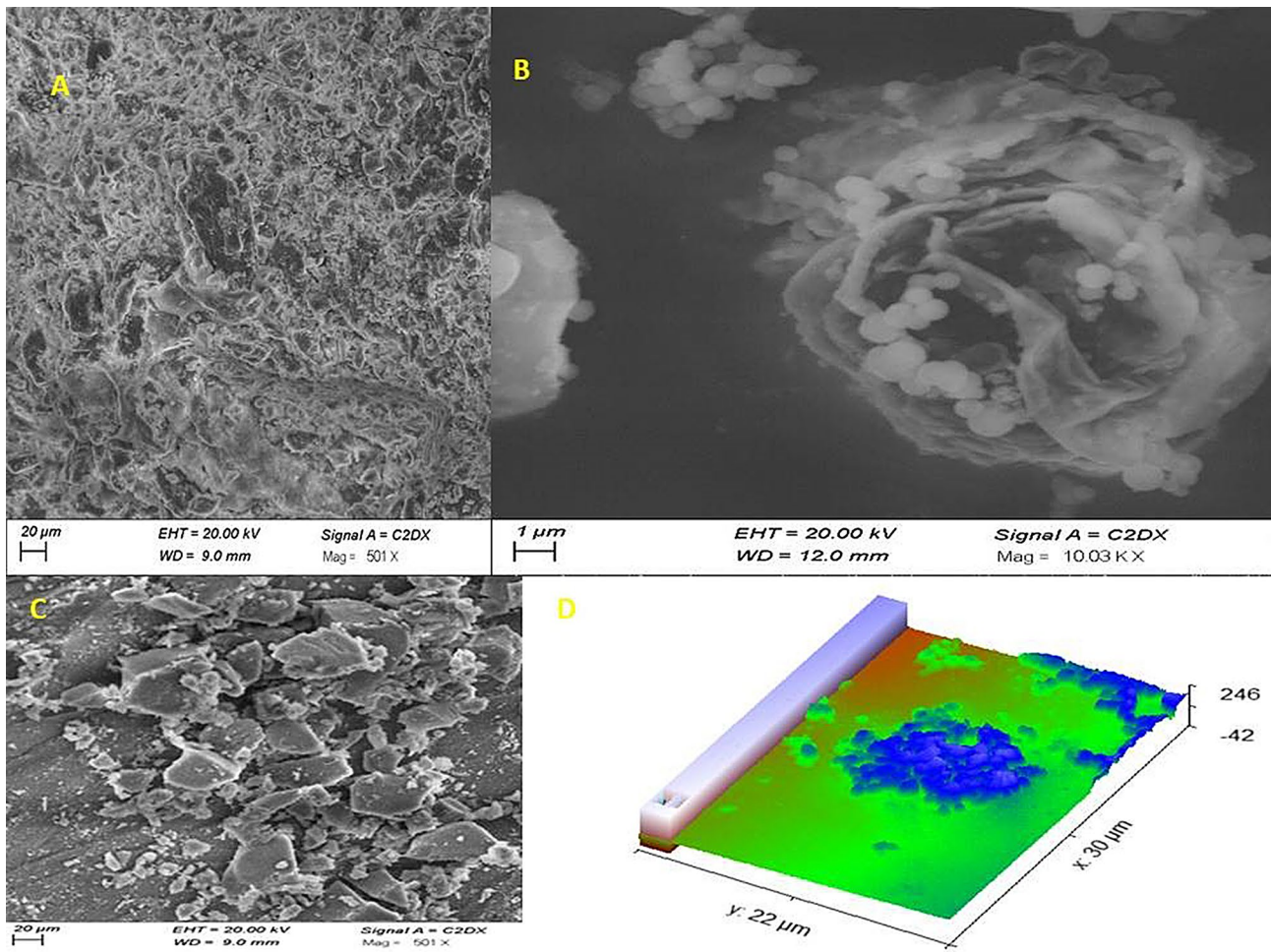


Fig. 4 Images of the CXP nano spray (A and B), the CXP pure drug (C) and the AFM image of the CXP nano spray (D)

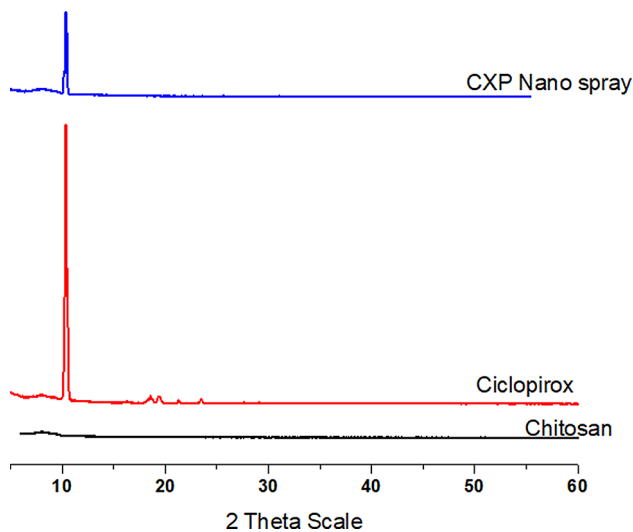


Fig. 5 XRD patterns of pure CXP, CS, and CXP nano spray

X-ray diffraction (XRDP)

X-ray diffraction (XRD) revealed the internal structures of the CXP nano spray, CS, and CXP pure drug crystals. The physical and chemical properties of the active ingredient determine the extent to which these changes occur. The XRD patterns for the CXP, CS, and CXP nano spray are displayed in Fig. 5. Crystalline peaks are observed via CXP XRD. There were noticeable peaks in the polymorphic XRD patterns observed at 2theta values of 90, 57, 54, 45, 90, 86, 41, 51, and 46. However, no clear peaks were observed in the CXP nano spray to support the transformation of CXP into an amorphous state, likely because of the increased pore confinement with the polymer matrix. Several faint peaks at 2theta 57, 46, 38, 41, 51, and 46 indicated the presence of CXP in an amorphous state inside the polymeric system. Both the CXP nano spray and CXP profiles were quite similar, and the CXP reflection peaks were still visible, indicating that CXP was partially retained in the nano spray.

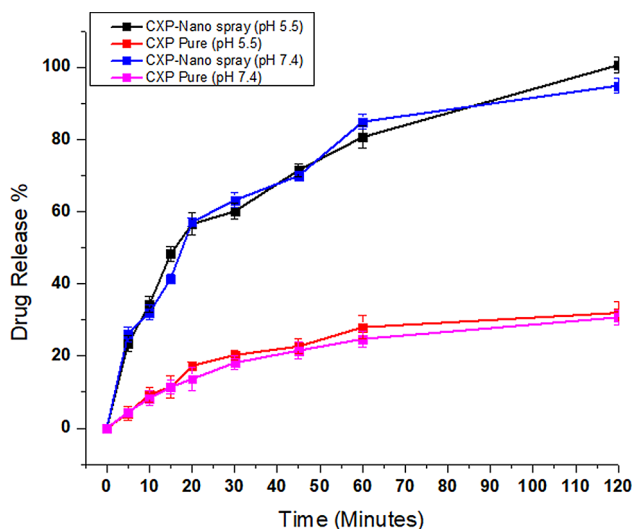


Fig. 6 In vitro drug release profile of the pure drug and formulation studied in (a) phosphate buffer at pH 5.5 and (b) pH 7.4 according to the dialysis bag membrane method ($n=3$)

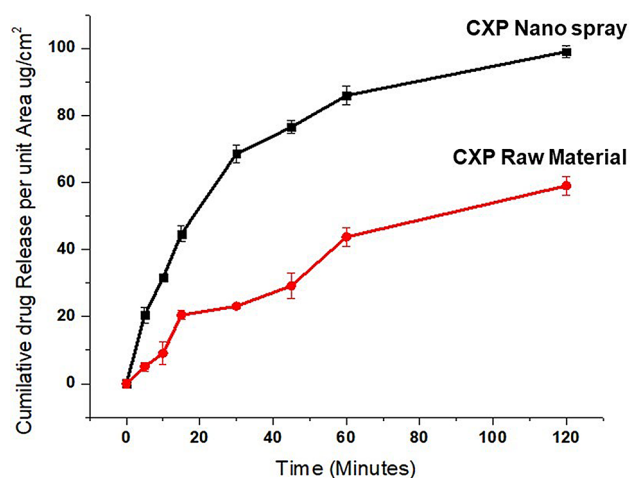


Fig. 7 In vitro permeability studies at pH 5.5

In-vitro release study

The dissolution of pure CXP and the CXP nano spray was examined in two buffers for 60 min. Figure 6 displays the profile form for both types of releases. The release profile of the CXP nano spray revealed an immediate release pattern that had two distinct phases, as shown in Fig. 6. The particle size of the CXP nano spray samples used in this study was 630 nm (PDI 0.295). This aids in enhancing the dissolution of the CXP nano spray in various media, leading to quick absorbance. The rate at which pure drugs are released is rather sluggish, taking up to 60 min for them to dissolve completely (given a water solubility of 1 mg/mL). The solubilities in both media exhibited strikingly similar patterns. The drug release pattern of the CXP nano spray gradually began in the first 10 min. However, it later shifted to a steady and uninterrupted drug release

pattern, leading to complete dissolution within 60 min in both buffers and pH levels, with dissolution rates of 100% and 97%, respectively. The rate of particle dissolution varied with size, as illustrated in Fig. 7. This discovery highlights the efficacy of the method in distinguishing between different materials.

In vitro permeability

The primary objective of this study was to examine the transcellular permeability of a nano spray with various pH values across a silica membrane in a controlled laboratory setting. The buffer solution was used to fill the receptor cell, which was thoroughly cleaned and dried. The mixture was allowed to rest for 15 min in a heated magnetic block at 37 °C. A hydrated silica membrane (artificial skin) was utilized to separate the donor and receptor compartments, with the indoor compartment housing 0.1 g of nano spray. The openings were carefully sealed with parafilm to ensure that evaporation was minimized. The stirring speed of the receptor compartment remained constant at 200 rpm. A 0.5 ml final sample was collected via a glass syringe for analysis on an HPLC at a wavelength of 298 nm. To maintain the uniformity of the sample volume in the receptor compartment, a fresh sample of the same volume was reintroduced after being warmed beforehand. According to the findings presented in Fig. 8, the formulation exhibited a significantly extended delivery time in comparison with the commercial cream, as evidenced by the in vitro permeation studies. These results indicate that this system has significant potential for drug delivery systems.

Hemolysis investigations

We performed hemolytic studies to investigate the compatibility of the CXP nano spray with rat blood. After conducting thorough hemolytic analyses, it was determined that the CXP nano spray, when used at concentrations of 100, 150, and 200 mg mL⁻¹, did not cause hemolysis. Despite the highest concentration of 200 mg mL⁻¹, only a minimal level of hemolysis (5.353, 9.173, and 13.25%) was observed in the experiment. Blood cells clearly demonstrate impressive resilience to intricacy (R^2 0.9953). On the basis of the findings of the latest study (Fig. 9), the concentration clearly had a notable effect on the viability of the cells. Through meticulous observation, it was revealed that cells retained their vitality even when exposed to the CXP nano spray. This discovery offers compelling evidence of the compatibility of the substance with human blood (Fig. 9).

In vitro cell viability testing

The cells were placed in 96-well plates at a density of 5×10^3 cells/well and allowed to grow overnight. The cells were then exposed to different concentrations ranging

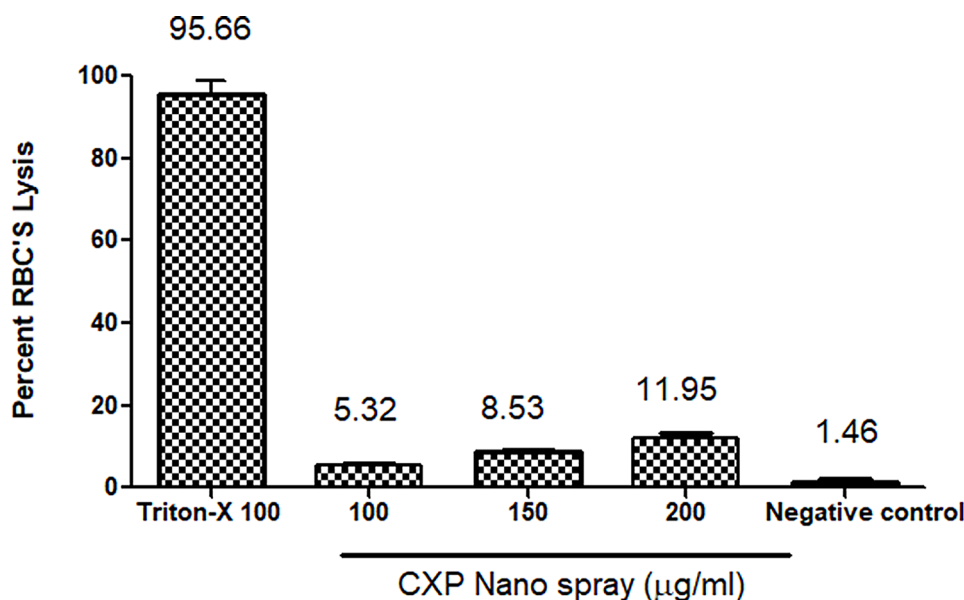


Fig. 8 Compatibility of CXP nano spray with blood

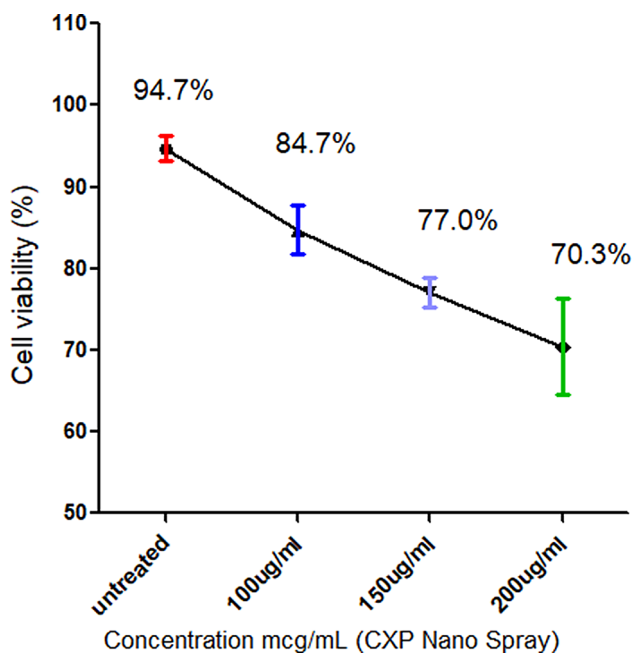


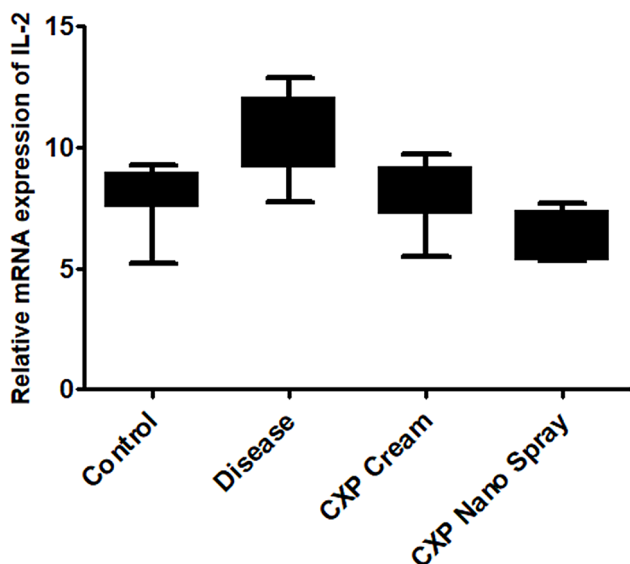
Fig. 9 Percent viability at 100, 150, and 200 µg/mL CXP nano spray

from 50 to 1000 mcg/ml. A study was carried out using a human hepatoma cell line (HepG2) at various concentrations. The samples consisted of untreated samples at different concentrations (100, 150, 200, 400, and 1000 µg/mL). The cells were incubated for 24 h at a carefully regulated room temperature. The Image Xpress Micro from Molecular Devices captured fluorescence images of five random fields in each well. The cell count was normalized in the untreated group, and there were no indications of any toxicity at any of the concentrations of the CXP nano spray. The CXP nano spray concentration in water

(untreated cells) is highly safe and compatible with biological systems. We analyzed cell viability with different concentrations of CXP nano spray (100, 150, 200, 400, and 1000 µg/mL). The findings revealed a distinct correlation between the dosage and the extent of cell toxicity. The range of cell viability values observed was from 0.921 ± 0.36 to 0.462 ± 0.07 µg/mL, suggesting a pattern that is dependent on the dosage. These findings suggest that the toxicity of the CXP nano spray is not significant. Following 24 h of exposure in HepG2 cells, the CXP nano spray had an IC50 of 902.35 µg/mL, suggesting its relatively low toxicity (Fig. 8).

Effect of CXP nano spray on the IL-2 mRNA expression level

The data revealed that the levels of IL-2 mRNA expression were greater in the disease group than in the control group. When the sick group and the treatment group were analyzed, a notable decrease in the level of IL-2 mRNA expression was observed when CXP nano spicks and pure drugs were used. Four groups were utilized in this experiment, with the diseased group being subjected to the disease-causing agent for a period of 28 days (Fig. 10). The control group of mice with allergic rhinitis was not subjected to any chemical interventions for 28 days. Two more groups were involved in the study and received an OVA solution administration. After a 14-day period of OVA exposure, both groups received CXP nano spray or pure drug. There was a noticeable decrease in the mRNA level of IL-2 in groups III and IV compared with that in group II (diseased) (6.781 ± 0.117 vs. 5.386 ± 0.189). Nevertheless, a noticeable distinction was noted between Group III and Group IV in comparison to the diseased group. Compared with those in



Comprasion of CXP cream and CXP Nano spray on IL-2 mRNA Expression Level

Fig. 10 Effects of CXP alone and CXP nano spray on the IL-2 mRNA expression level

Table 2 Optimized formulation of the CXP nano spray

Sr. #	Material Name	Quantity of Material Used	Percentage (%) of Material
1.	Ciclopirox	100 mg	0.66%
2.	Chitosan	500 mg	0.66%
3.	Ethanol	10 mL	26.0%
4.	Tween-80	1.0 mL	3.53%
5.	Water	100 mL	65.80%
Total			99.95%

the control group, the mRNA levels of IL-2 in the group treated with the CXP nano spray significantly decreased, similar to the results of the control group. This phenomenon can be attributed to the rapid absorption of the spray in the blood and lungs of the mice. This study revealed

that, compared with the pure drug, the CXP nanospray is promising for treating fungus infections.

Significant reduction in TLC and DLC in the blood by the CXP nano spray

Four groups of mice were subjected to blood analysis: a control group, a group with a disease, a group treated with a CXP nano spray, and a group treated with the pure drug. The mice in the control group were given a standard phosphate buffer solution for a duration of 28 days. The remaining three groups were subjected to an ovalbumin challenge. Following a two-week period, the two groups began treatment with the experimental medications, while the groups impacted by the disease were exposed to OVA for a total of 28 days. Blood samples revealed that the disease group presented significantly higher levels of total leucocytes, lymphocytes, neutrophils, monocytes, and eosinophils than did the control group. Compared with those of the control group, the blood of the sick group of mice was significantly increased in different types of white blood cells, including leucocytes, lymphocytes, neutrophils, monocytes, and eosinophils (all P values 0.001). After the CXP nano spray was applied, a noticeable decrease ($p < 0.001$) in the DLC was observed in comparison with that in the group that received only the pure drug (Table 2). These results suggest that the CXP nano spray has a notable effect on decreasing or eliminating the TLC and DLC parameters in mice with diseases.

Antifungal study

The Sabouraud dextrose agar (SDA) well diffusion technique was used to assess the antifungal activity of the hydrogel films against *Aspergillus* mold in vitro. The inhibitory zones for the CXP nano spray formulation and W.S. are shown in Fig. 11. The results showed that the CXP nano spray was highly effective against fungi and had excellent antifungal properties. These results are consistent with those of previous studies. The synergistic

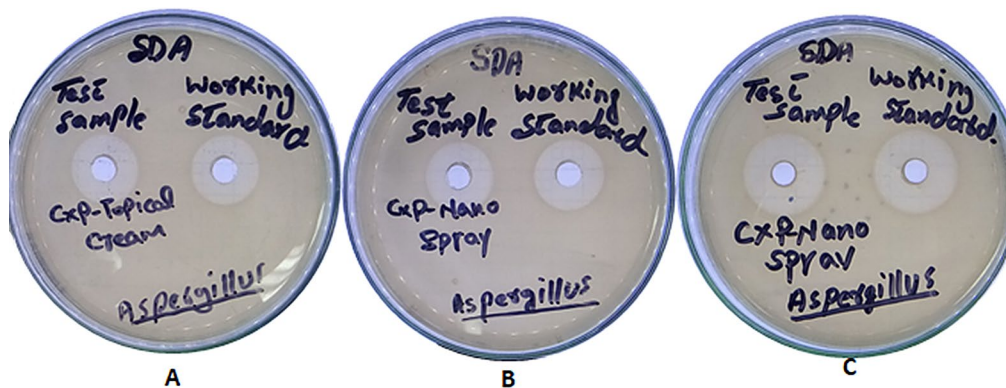


Fig. 11 Image of the antifungal inhibition zones for CXP nanospray (TS) and the working standard

Table 3 Mean \pm SD of TLC and DLC in the blood of all the groups ($n = 3$)

Parameters (Blood)	Group I (Control)	Group II (Disease)	Group III CXP nano spray	Group IV Pure dug
TLC 1000/uL	6.2 \pm 1.53	11.28 \pm 1.73	8.04 \pm 1.29	6.92 \pm 0.52
Lymphocytes %	4.9 \pm 0.56	5.9 \pm 0.1	4.2 \pm 0.17	3.5 \pm 0.14
Neutrophils %	1.16 \pm 0.08	2.5 \pm 0.56	1.35 \pm 0.12	1.7 \pm 0.35
Eosinophils %	0.18 \pm 0.04	0.27 \pm 0.09 ^a	0.19 \pm 0.09	0.43 \pm 0.012
Monocytes %	0.24 \pm 0.11	0.97 \pm 0.01	0.31 \pm 0.11	0.79 \pm 0.03
Basophils %	0.05 \pm 0.009	0.12 \pm 0.002	0.03 \pm 0.009	0.12 \pm 0.031

Table 4 Zone of inhibition of nanospoil and working standards
Zone of inhibition (mm)

Assay #	Working standard solution	CXP nano spray Test Solution
1	18.22	19.94
2	18.62	19.72
Average	18.42	19.83
% Assay	Limit % 90–110	
% assay of Ciclopirox	98.99% \pm 2.00%	

Table 5 Microbial limit test results according to USP 43

Description	Results (cfu/mL)			Limits
	Batch # 001	Batch # 002	Batch # 003	
Total Aerobic Microbial Count (TAMC)	< 10 cfu/mL	< 10 cfu/mL	< 10 cfu/mL	200 cfu/mL
Total Combined Yeasts & Molds Count (TYMC)	< 10 cfu/mL	< 10 cfu/mL	< 10 cfu/mL	20 cfu/mL
Tests for Absence of specified Microorganisms				
<i>Staphylococcus aureus</i>	Absent/mL	Absent/mL	Absent/mL	Should be absent/mL
<i>Pseudomonas aeruginosa</i>	Absent/mL	Absent/mL	Absent/mL	Should be absent/mL

interaction between CS and CXP explains the antifungal effects of the nanospray. Chemical species (CSs) can interact with different types of cell membranes because their amino group chains can protonate into NH_3^+ and become cationic when dissolved in an acidic environment. The antifungal effects of chitosan are mostly due to its positive charge. It inhibits the ability of fungi to act or kill by interacting with their negatively charged cell membranes. Compared with W.S., the CXP nano spray had a larger zone of inhibition against *Aspergillus*, measuring 19.83 mm in diameter (Table 3).

Table 6 Compression parameters of the prepared nano spray and commercial products

Formulation	Clarity	pH	Homogeneity	Viscosity cpi
CXP nano spray	Clear	6.1 \pm 0.5	Good	79 \pm 0.8
Commercial product	Clear	6.8 \pm 0.6	Good	69 \pm 1.6

Microbiological studies (antifungal study)

For the nano spray formulation of the CXP nano spray to be approved for patient use, it must first fulfill all microbiological parameters and USP 43 requirements. Testing for TAMC, TYMC, *Staphylococcus*, and *Pseudomonas* was conducted following the scaling up of the formulation. We counted the number of colony-forming units (CFUs) on plates via the gold standard approach (Table 4). To produce plates, scientists have utilized Sabouraud dextrose agar and nutrient agar [40]. Different temperatures (32 ± 2 °C and 22 ± 2 °C) were used to incubate the plates in Memmert incubators for 72 h for the TAMC and seven days for the TYMC. Table 5 displays the results.

Physical characterization

A liquid formulation of CXP nano spray was developed for use in nano spray applications. The formulation for the CXP nano spray has a pH of 6.1 ± 0.5 , which is appropriate for skin products, as per the USP. The skin usage of the formulation is also supported by its viscosity of 79 ± 0.8 cpi at 25 °C. Both goods were determined to have adequate levels of homogeneity and clarity (Table 6).

Conclusion

Research conducted in this study indicates that an optimized formulation of CXP nanospray might be useful in the treatment of fungus. As far as we are aware, this is the initial documentation of a topical medication delivery system utilizing CXP and a nanoprecipitation-based formulation. The physicochemical properties, loading content, and drug encapsulation efficiency of the successfully manufactured CXP nanospray were satisfactory. The results from both in vitro and in vivo toxicity studies showed that CXP nanospray was safe for usage around blood and organs, and it did not cause any noticeable harm to cells. More in vitro and in vivo studies are needed to confirm our suspicions that topical absorption of CXP nanospray is a viable option for improving local therapy of fungus. The formulation is quite stable and may be simply scaled up. Now that we have these novel CXP delivery methods, we need to do stability evaluations, pharmacokinetic studies (both in the lab and in humans), investigations of patient usability and acceptance, and models of pharmacokinetics based on physiological principles.

Acknowledgements

The authors extend their appreciation to the Researchers Supporting Project number (RSP2025R189) King Saud University, Riyadh, Saud Arabia.

Author contributions

Conceptualization, original draft writing, reviewing, and editing: Yasir Mehmood, Hira Shahid, Rabbia Nazir. Formal analysis, investigations, funding acquisition, reviewing, and editing: Mohammad N. Uddin, Mohammad Nur-e-Alam, Mohsin Kazi. Resources, data validation, data curation, and supervision: Mohammed Bourhia, Khalid S. Almaary, Ousman B. Mahamat.

Funding

This work is supported by the Researchers Supporting Project number (RSP2025R189), King Saud University, Riyadh, Saudi Arabia.

Data availability

The datasets used and/or analyzed during the current study are available from the corresponding author upon reasonable request.

Declarations

Ethics approval and consent to participate

Protocol was approved by the Ethical Review Board of the Ethical Committee of Riphah International University Faisalabad under ethical number IRB NO: RLC/197/2023). Notably, all animal experimentation was conducted in accordance with applicable laws, regulations, and guidelines, prioritizing animal welfare and minimizing any potential harm.

Consent for publication

Not applicable.

Clinical trial number

Not applicable.

ARRIVE guidelines

The experimentation was conducted in accordance with applicable laws, and ARRIVE guidelines.

Competing interests

The authors declare no competing interests.

Author details

¹Riphah Institute of Pharmaceutical Sciences (RIPS), Riphah International University Faisalabad, P.O. Box 38000, Faisalabad, Pakistan

²Department of Pharmacology, Faculty of Pharmaceutical Sciences, Government College University Faisalabad, P.O. Box 38000, Faisalabad, Pakistan

³University College of Pharmacy, University of the Punjab, Allama Iqbal Campus, Lahore, Pakistan

⁴College of Pharmacy, Mercer University, Atlanta, GA 30341, USA

⁵Department of Pharmacognosy, College of Pharmacy, King Saud University, PO BOX-2457, Riyadh 11451, Saudi Arabia

⁶Laboratory of Biotechnology and Natural Resources Valorization, Faculty of Sciences, Ibn Zohr University, Agadir 80060, Morocco

⁷Department of Botany and Microbiology, College of Science, King Saud University, P. O. BOX 2455, Riyadh 11451, Saudi Arabia

⁸Department of Pharmaceutics, College of Pharmacy, King Saud University, P.O. Box 11451, Riyadh, Saudi Arabia

⁹National Federation of Associations of Medical Practitioners in Chad (FENAPMT), Ministry of Health, N'Djamena, N'Djamena City, Republic of Chad

¹⁰Faculty of Science, University of Abdelmalek Essaâdi, Tetoun, Morocco

References

1. Vikas A, et al. Mechanistic insights of formulation approaches for the treatment of nail infection: conventional and novel drug delivery approaches. *AAPS PharmSciTech*. 2020;21:1–12.
2. Mishra V, et al. Nanoarchitectures in management of fungal diseases: an overview. *Appl Sci*. 2021;11(15):7119.
3. Keshwania P, et al. Superficial dermatophytosis across the World's populations: potential benefits from Nanocarrier-based therapies and Rising challenges. *ACS Omega*. 2023;8(35):31575–99.
4. Abd-El salam WH, Abouelatta SM. Contemporary techniques and potential transungual drug delivery nanosystems for the treatment of onychomycosis. *AAPS PharmSciTech*. 2023;24(6):150.
5. Farheen F, et al. Updated perspectives on the diagnosis, Management and novel drug delivery strategies for the treatment of onychomycosis. *J Pharm Negat Results*, 2022; pp. 3669–90.
6. Srivastava R, et al. Advancements in nanotechnology for enhanced Antifungal Drug Delivery: a Comprehensive Review. *Infect Disorders-Drug Targets (Formerly Curr Drug Targets-Infectious Disorders)*. 2024;24(2):24–36.
7. Bayat F, et al. Nanostructured drug delivery approaches for fungal infections. *Emerging nanomaterials and Nano-based drug delivery approaches to Combat Antimicrobial Resistance*. Elsevier; 2022. pp. 179–232.
8. Behera JK, et al. Novel discoveries and clinical advancements for treating onychomycosis: a mechanistic insight. *Adv Drug Deliv Rev*, 2023; p. 115174.
9. G Ramu B, et al. A review on SLN and NLC for management of fungal infections. 2021.
10. Tampucci S, et al. Formulations based on natural ingredients for the treatment of nail diseases. *Curr Pharm Design*. 2020;26(5):556–65.
11. Sethi SK, Goel H, Chawla V. Nanoemulsion Based Supramolecular Drug Delivery systems for Therapeutic Management of Fungal infections. *Drug Delivery Lett*. 2024;14(1):2–15.
12. Ahuja A, Bajpai M. Nanoformulations insights: a Novel paradigm for antifungal therapies and future perspectives. *Current Drug Delivery*; 2023.
13. Abdalla A, El-Sawy HS, Ramadan AA. Emergence of Advanced Antifungal-Delivery approaches for the treatment of Tinea Pedis. *ERU Research Journal*; 2024.
14. Gholami-Shabani M, et al. Fungal biofilms in nanotechnology era: diagnosis, drug delivery, and treatment strategies. In: *Myconanotechnology*. CRC Press; 2023. p. 129–168.
15. Kaur N, et al. A review on antifungal efficiency of plant extracts entrenched polysaccharide-based nanohydrogels. *Nutrients*. 2021;13(6):2055.
16. Aderibigbe BA. Nanotherapeutics for the delivery of antifungal drugs. *Therapeutic Delivery*. 2024;15(1):55–76.
17. Chuah L-H, et al. Chitosan-based drug delivery systems for skin atopic dermatitis: recent advancements and patent trends. *Drug Delivery Translational Res*. 2023;13(5):1436–55.
18. Reddy A, Sureshkumar R. An insight of emerging role of nanotechnology for the management of athlete's foot. *Int J Pharm Res*. 2021;13(1). (09752366).
19. Harak PD, Zalte AG, Gulecha VS. Formulation and evaluation of film forming solution of tavorole for treatment of skin infections. *Res J Pharm Technol*. 2023;16(3):1342–6.
20. Ferreira L, et al. Cyclodextrin-based dermatological formulations: dermopharmaceutical and cosmetic applications. *Colloids Surf B*. 2023;221:113012.
21. Aggarwal R, et al. Treatment and management strategies of onychomycosis. *J De Mycol Medicale*. 2020;30(2):100949.
22. Ullah KH, et al. Chitosan nanoparticles loaded poloxamer 407 gel for transungual delivery of terbinafine HCl. *Pharmaceutics*. 2022;14(11):2353.
23. Sharma A, Gupta S. Protective manifestation of herbonanocentials as antifungals: a possible drug candidate for dermatophytic infection. *Health Sci Rep*. 2022;5(5):e775.
24. Mehmood Y, et al. In-vitro and in-vivo evaluation of velpatasvir-loaded mesoporous silica scaffolds. A prospective carrier for drug bioavailability enhancement. *Pharmaceutics*. 2020;12(4):307.
25. Mehmood Y, et al. Amino-decorated mesoporous silica nanoparticles for controlled sofosbuvir delivery. *Eur J Pharm Sci*. 2020;143:105184.
26. Mahajan A, et al. Multipotentiality of Luliconazole against various fungal strains: Novel Topical formulations and Patent Review. *Recent Adv Anti-Infective Drug Discovery Former Recent Pat Anti-Infective Drug Discovery*. 2021;16(3):182–95.
27. Mehmood Y, et al. Facile synthesis of mesoporous silica nanoparticles using modified solgel method: optimization and In Vitro cytotoxicity studies. *Pak J Pharm Sci*. 2019;32(4):1805–12.

Received: 28 November 2024 / Accepted: 22 January 2025

Published online: 14 February 2025

28. Kaur, N., et al. A review on antifungal efficiency of plant extracts entrenched polysaccharide-based nanohydrogels. *Nutrients*. 2021;13(2055). 2021, s Note: MDPI stays neutral with regard to jurisdictional claims in published...
29. Faustino C, Pinheiro L. Lipid systems for the delivery of amphotericin B in antifungal therapy. *Pharmaceutics*. 2020;12(1):29.
30. Barkat K, et al. Development and characterization of pH-responsive polyethylene glycol-co-poly (methacrylic acid) polymeric network system for colon target delivery of oxaliplatin: its acute oral toxicity study. *Adv Polym Technol*. 2018;37(6):1806–22.
31. Khalid I, et al. Preparation and characterization of alginate-PVA-based semi-IPN: controlled release pH-responsive composites. *Polym Bull*. 2018;75(3):1075–99.
32. Thakur S, et al. Thermosensitive injectable hydrogel containing carboplatin loaded nanoparticles: a dual approach for sustained and localized delivery with improved safety and therapeutic efficacy. *J Drug Deliv Sci Technol*. 2020;58:101817.
33. Abdul AH, et al. Equator Assessment of nanoparticles using the Design-Expert Software. *Int J Pharm Sci Nanotechnol*. 2020;13(1):4766–72.
34. Wu S, et al. Progress of polymer-based strategies in fungal disease management: designed for different roles. *Front Cell Infect Microbiol*. 2023;13:1142029.
35. Hosseinpour-Moghadam R, et al. Applications of novel and nanostructured drug delivery systems for the treatment of oral cavity diseases. *Clin Ther*. 2021;43(12):e377–402.
36. Chakraborty T, et al. Wound healing potential of insulin-loaded nanoemulsion with Aloe vera gel in diabetic rats. *J Drug Deliv Sci Technol*. 2021;64:102601.
37. Hammoudi Halat D, et al. Allylamines, benzylamines, and fungal cell permeability: a review of mechanistic effects and usefulness against fungal pathogens. *Membranes*. 2022;12(12):1171.
38. AbouSamra MM, et al. Synergistic approach for acne vulgaris treatment using glycosomes loaded with lincomycin and lauric acid: Formulation, in silico, in vitro, LC-MS/MS skin deposition assay and in vivo evaluation. *Int J Pharm*. 2023;646:123487.
39. Phadtare DG, Gaika MN, Aher SS. Formulation and characterization of nano-emulsion based nasal spray of azelastine hydrochloride. *Res J Topical Cosmet Sci*. 2016;7(2):55.
40. Marena GD, et al. Natural product-based nanomedicine applied to fungal infection treatment: a review of the last 4 years. *Phytother Res*. 2022;36(7):2710–45.

Publisher's note

Springer Nature remains neutral with regard to jurisdictional claims in published maps and institutional affiliations.